1   Long-term visibility variation at the Ebro Observatory (1960–2020).

3   Juan José Curto [(1)], Nicolás Tacoronte [(1,2)]
4   (1)   Observatorio del Ebro, (OE) CSIC – Universitat Ramón Llull
5   (2)   Universidad Complutense de Madrid

7   Corresponding author: J.J. Curto (jjcurto@obsebre.es)

9   Abstract.
10   This study explores the interdecadal variability and trends of surface horizontal visibility in the Baix Ebre area
11   (Spain) from 1960 to 2020, using the historical archive of the Ebro Observatory located in the town of Roquetes,
12   in the centre of the region. We detected a prominent improvement in visibility in the first decades of the second
13   part of the twentieth century but this was followed by a dramatic deterioration in the last decade recorded
14   (2010-2020). This was not accompanied by a significant trend in relative humidity over the same period. It was
15   found that very good visibility (20-50 km) occurred at a frequency of more than 40% in the 1980s and 90s, while
16   this percentage dropped to just 15% during the 2010–2020 decade.
17   Visibility was found to be negatively correlated with relative humidity and positively correlated with wind speed.
18   This correlation was statistically valid for most of the time periods we looked at. Wind regime, prevailing wind
19   direction and the corresponding origin (marine or continental) of the air mass were found to display a strong
20   influence on the short-term visibility levels at the Ebro Observatory. However, long term visibility trends are
21   controlled by other factors, which are probably of anthropogenic origin. The rapid increase in population in
22   Roquetes and other neighbouring towns during recent decades could be the cause of the implicit impairment of
23   air quality observed because of increased levels of air pollution on a regional scale. Apart from these local
24   sources, visibility at the Ebro Observatory could also be influenced by the aerosol load from neighbouring regions
25   (Castelló and Tarragona) which have a significant concentration of industries.

28   Keywords: visibility, humidity, wind, interdecadal variability.

31   1. Introduction.

33   Atmospheric visibility is defined as the maximum distance a black object of suitable
34   dimensions (located close to the ground) can be seen and recognized when viewed against a
35   sky background during the day or the distance it could be seen and recognized at night at if
36   the general lighting was raised to the normal daytime level (World Meteorological Organization
37   [WMO], 1992). It represents one of the dominant features of the climate and landscape of an
38   area (Founda et al., 2016). Three fundamental factors make visibility measurements difficult
39   to carry out: local meteorology, the physiology of the human eye and, finally, the
40   characteristics of the object to be viewed with respect to the surrounding background.

42   Many studies have been performed on rural and urban areas in different countries, e.g. Taiwan
43   (Tsai, 2005), United Kingdom (Doyle and Dorling, 2002), China (Deng et al., 2012), India (Hu,
44   2017), United States (Sloane, 1982), Iran (Sabetghadam, 2012), Hungary (2008) and Greece
45   (Founda et al., 2016). The main objective of our study is to understand the changes that have
46   occurred in atmospheric visibility from 1960 to the present day at the Ebro Observatory, a
47   Spanish observatory with a long history of records. To do this, we analysed the annual and
48   seasonal variability of the visibility. Data were grouped using different scales, such as those
49   recommended by the World Meteorological Organization (WMO), but in some parts of this
50   study, other *adhoc* adapted classifications were used with the recorded values. We checked
51   how the trends in the observations vary for different periods of time. The records of relative

52 humidity and the wind regime were also studied, examining the relationships between these
53 variables and visibility.

2. Location.

2.1. Area of study.

56

57 The Ebro Observatory (40.8 ° N, 0.5 ° E) is located in the Eastern quadrant of the Iberian
58 Peninsula (Figure 1). It is a centre devoted to geophysical observations. It works in
59 coordination with the National Meteorological Agency (AEMET), and, in addition, it
60 collaborates with other official and private organizations in the same line of research. It was
61 founded in 1904 with the aim of studying the relationships between the Earth and the Sun
62 (Cirera, 1906; Puig, 1927; Cardús, 1983). Since then, a wide variety of records of great
63 scientific value have been accumulated, such as magnetic, ionospheric and seismic archives,
64 which are considered to make up one of the most extensive collections of data in Spain. In
65 fact, our meteorological archives date back to the year 1880. As a result of this, we have a
66 long series of meteorological data that allows us to carry out climate studies of the Ebro and,
67 by extension, the Mediterranean region (Curto et al., 2008). Among all these data, there is a
68 historical series of atmospheric visibility. The last sixty years of these records have been
69 digitized and we have worked with them analysing trends and relationships with
70 meteorological variables and also with other effects linked to human activity (Curto et al.,
71 2008).

72
73 Figure 1: Topographic map showing the location of the Ebro Observatory (black dot) at the end of the Ebro
74 Valley, close to the Ebro river delta and the Mediterranean Sea. The red circle describes the mean distance
75 achieved with visibility observations.

76
77

78 The data from the Observatory's meteorological stations are particularly suitable for
79 ascertaining the existence of possible climatic changes or fluctuations, as it is an observation
80 point that has never moved nor experienced significant changes in its surroundings from 1910
81 onward (Raso, 1987).

82 ## 2.2. Climatic characteristics of the site.

83
84 The Ebro basin includes a gradient from Atlantic to Mediterranean climates, and has complex
85 topography, geology and land cover (López-Moreno et al., 2013). This heterogeneous
86 topography and the influence of various large-scale atmospheric patterns, like the North
87 Atlantic Oscillation, the Mediterranean Oscillation and the Western Mediterranean Oscillation
88 (Vicente-Serrano et al., 2009; Vicente-Serrano and Lopez-Moreno, 2006) generate a complex
89 spatial distribution of climate parameters (López-Moreno et al., 2011).

90
91 Specifically, for this area, the climate is mild in general. The air temperature rarely drops to
92 zero degrees and hardly ever rises above 34ºC, resulting in a moderate and temperate series
93 of values. The depressions of the Mediterranean produce strong winds, although not cold,
94 which are channelled by the Ebro valley (Figure 1). The NNW wind predominates in the winter
95 months and the SSE breeze predominates in summer (Cirera, 1910).
96

97 # 3. Data and methodology.

98
99   The visibility data have been continuously measured at the same site with a surface weather
100 station. We worked with the data corresponding to atmospheric visibility, wind speed and
101 direction and relative humidity. We focused on the 07:00 LT, 13:00 LT, and 18:00 LT
102 observations as being representative for morning, noon, and afternoon or evening conditions.

103
104 The available visibility data were taken by specialized observers and entered in notebooks by
105 hand. Rotating shifts involved different observers so any hypothetical personal bias was
106 compensated for. Regarding our data analysis, first of all, it was necessary to locate the
107 existence of gaps and outliers that may contribute to errors in the results. With this in mind, a
108 code was created that separates the days for which no data were found and also detects those
109 cases that are considered to present a problem with the aim of trying to solve it. The criterion
110 used consists in eliminating those values greater than 1.5 times the interquartile range below
111 the first quartile and above the third for each hour of the day. However, the relative humidity
112 and wind speed and direction data were assumed to be valid *a priori* as they were measured
113 with instrumentation and were verified by a data manager.

114
115 To study the visibility variations, temporal averages were taken, using group divisions of years,
116 months or weeks. To study how the collected horizontal visibility data vary throughout the
117 study period, they were divided based on an empirical scale of visibility classes, as
118 recommended by the World Meteorological Organization, WMO (Wang et al. 2010). This scale
119 is displayed in Table 1.
120
121

122   Table 1: Visibility classes of WMO directive.
123

Class	1	2	3	4	5	6	7	8	9
Visibility (km)	0.050-0.2	0.2-0.5	0.5-1	1-2	2-4	4-10	10-20	20-50	>50

124
125
126   On the other hand, a similar study was carried out with the wind direction and intensity data,
127   and so diagrams were obtained representing the frequency with which winds from a certain
128   direction occurred depending on the time of year. It is also possible to relate these data to the
129   recorded atmospheric visibility measurements. In this way, the representations of the visibility
130   variations were obtained as a function of the sectors from which the wind comes, or by relating
131   the wind speed to the direction from which the wind comes from.
132
133   Finally, the correlation coefficient between visibility and relative humidity or wind was
134   calculated.
135

136   ## 4. Results.

137   ### 4.1. Variations in the visibility.

138
139   It can be verified that visibility presented gradual variations throughout most of the years in
140   the last century (Founda et al., 2016), but, at the Ebro Observatory, a significant and more
141   abrupt increase appeared in the decade 1980-1990, followed by a subsequent decrease that
142   became even more abrupt in the last decade recorded (2010-2020) (Figure 2). On a global
143   scale, Wang & Liang (2009) showed a decrease in visibility between 1973 and 2007, which
144   was interpreted as being down to a higher concentration of aerosols and their impact on
145   incident solar irradiance. A significant decrease in visibility was observed in Asia, South
146   America, Australia and Africa, while in Europe visibility increased after the 1980s as a result
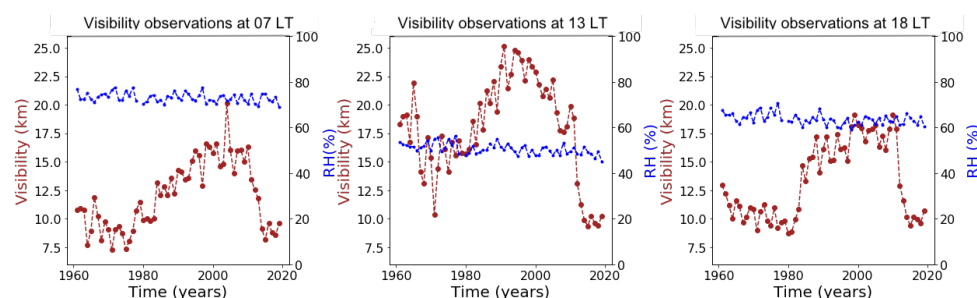147   of air pollution mitigation measures (Vautard et al., 2009).
148

150   Figure 2: Annual average of visibility (red dots) and relative humidity (blue dots) measurements between 1961
151   and 2019.
152
153   We also found it useful to study the monthly variation in visibility (Figure 3). The differences
154   that appeared between seasons may be due to certain factors such as the variation in relative

155 humidity throughout the year, since this may be indicative of precipitation or fog, which would
156 reduce visibility, or the recorded type of wind blowing in this area, which can clean the
157 atmosphere of suspended particles and pollutants leading to better visibility results, or to
158 worse results, depending on the area from which the wind blows.
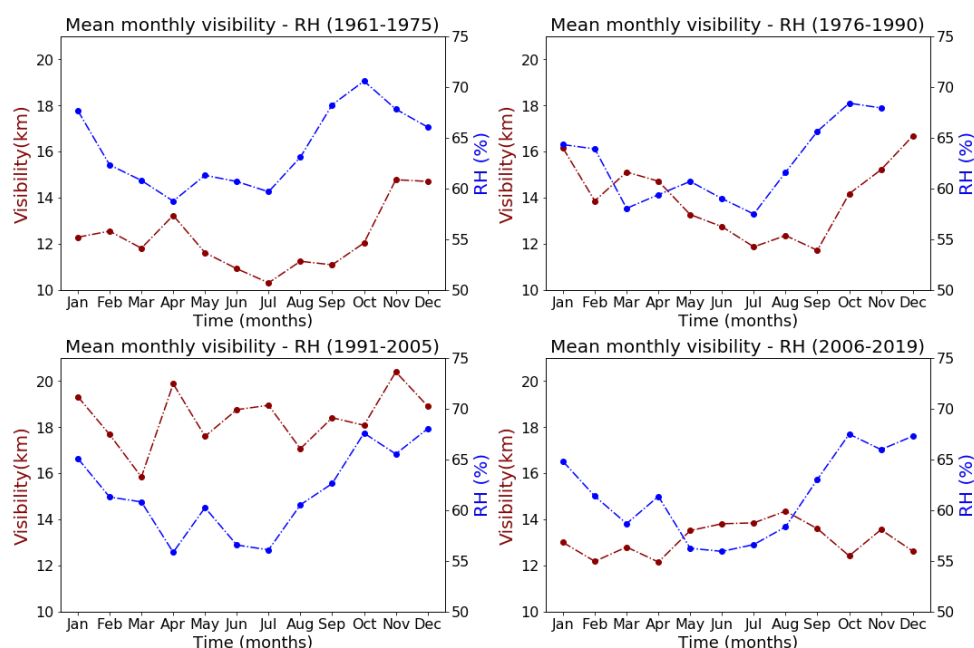
160 Figure 3: Average of monthly visibility (red line) and relative humidity (blue line) measurements between 1961
161 and 2019 in 15-year periods.

162

163 The results shown in Figure 3 indicate that, in general, the maximum average visibility was
164 found during the winter months and the minimum in July, August and September, except for
165 the last period of time measured. The correlation of these results with those of relative humidity
166 will be presented later, but from this representation it can already be seen that there is no clear
167 dependence between the two variables. With the average relative humidity values that have
168 been represented, the hypothesis that fog or precipitation are factors to be highlighted in the
169 global change in visibility can be ruled out.

170

171 Finally, to study how the horizontal visibility data vary throughout the studied period, we
172 grouped them according to the aforementioned empirical scale of visibility classes
173 recommended by the WMO (Wang et al. 2010).
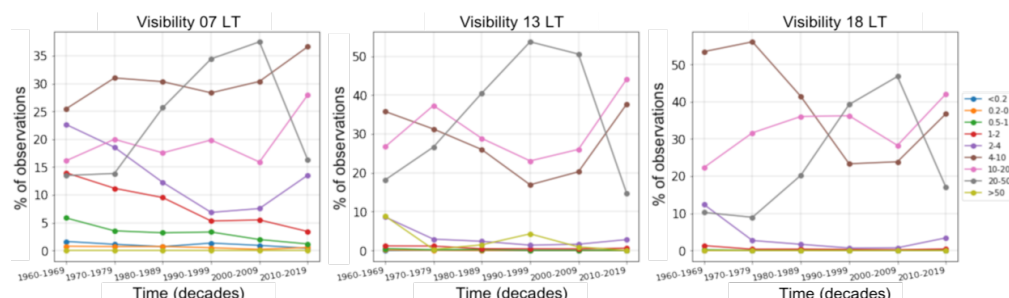
174

175

Figure 4: Temporal evolution of visibility for each decade according to the class scale defined by the WMO for 07:00 LT, 13:00 LT and 18:00 LT.

A remarkable increase in the visibility observations of the largest class with time can be appreciated in Figure 4. During the 1960s, the majority of observations fell into class 6, while in the period 2000-2010, the most frequent were class 8 ones. In the last decade, however, this trend changed, registering a greater number of class 7 observations. The minor class observations, on the other hand, make up a minority in the global computation and do not significantly affect the mean. As in the representation of Figure 2, here it can be observed that visibility had been increasing until 2010, when there was a clear decrease, of up to 10 km, noted in the average visibility.

4.2. Wind data study.

For the study of the wind, we took into account intensity and direction data. To characterize the wind, the wind speed recorded at 07:00 LT, 13:00 LT and 18:00 LT in each sector was studied, differentiating it into 3 large groups: less than 5 m/s, between 5 m/s and 10 m/s and greater than 10 m/s (Figure 5). It was also necessary to know the relationship between the sectors from which the wind came and the visibility as well as the time of the year in which the measurements were recorded in the different sectors.

Due to the local orography, there are two favoured directions for the wind. Winds are conditioned by the shape of this section of the Ebro basin: from the upper part of the region, the area is open to the Ebro basin and terrestrial winds (*mistral*, NW) have easy access, whereas for the lower part, the area is open to the delta of the Ebro river which is connected to the Mediterranean flow inlets (sea breeze, E and SE). This is linked to infrequent and not very persistent storms. The whole area is located facing away and far from the Atlantic storms associated with the *ábregos* winds (W and NW) (Pedraza and García, 2013).
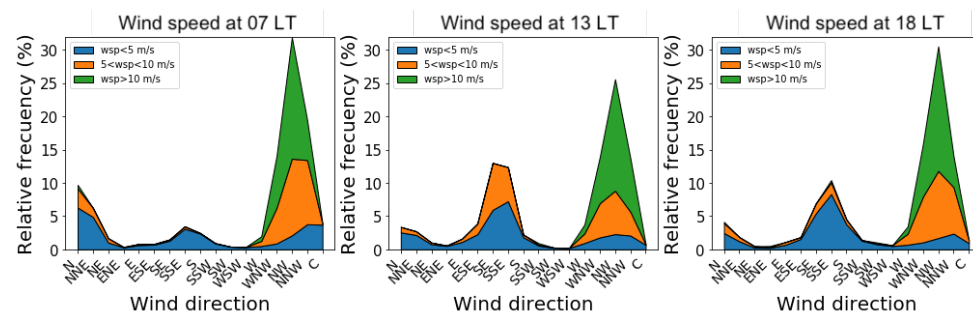
205 Figure 5: Relative frequencies of the number of measurements with respect to the surface wind directions for three
206 categories of wind speed (wsp). Soft (blue), medium (orange), and strong (green) at 07:00 LT (left), 13:00 LT
207 (centre), and 18:00 LT (right). Sector C refers to periods of calm (wsp <0.5 m/s).

208
209
210 The SSE-SSW sectors are linked to the transport of air masses from arid areas of North Africa,
211 frequently associated with dust events that affect wide areas of the Mediterranean. Temperate
212 and humid winds with a Mediterranean origin from here are less intense than the north wind
213 (Figure 5). There is an increase in the wind records for these southern winds at 13:00 LT due
214 to the influence of the sea breeze (Serrano et al. 2017). In Figure 7 it can be seen that the
215 wind coming from these regions is associated with minimum visibility and, as indicated in
216 Figure 6, it is more common to find it in summer. On the other hand, in the colder months,
217 stronger winds coming from the W-NW directions (Figure 6) are the prevailing ones. These
218 winds, called gale winds, are the ones that reach the highest speeds (Figure 5). They are cold,
219 dry, turbulent and are associated with maximum visibility (Figure 7).
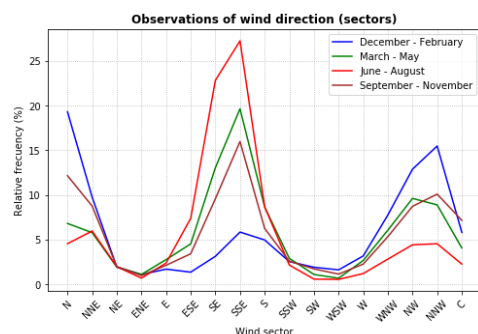
220

222 Figure 6: Visibility variation for each wind direction (sector) and for each season of the year.
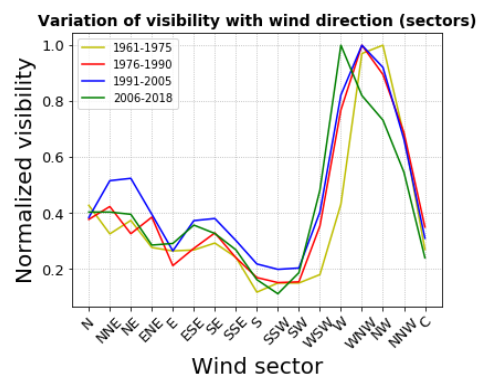223

225 Figure 7: Relative frequencies of the number of measurements recorded in each wind direction (sectors) during
226 different sub periods into which we have divided the series.

227 4.3. Correlation between atmospheric visibility and relative humidity /
228 wind.

229

230   Next, we studied to what extent visibility is affected by meteorological variables such as
231   relative humidity and wind, both of which could be classified as being of natural origin.
232
233   The clearest feature we found is that an increase in relative humidity causes a decrease in
234   visibility, as shown by the dominant negative correlations represented in Figure 8. According
235   to Lawal (2014), the relation:

$$t_{n-2} = \frac{r\sqrt{n-2}}{\sqrt{1-r^2}} \rightarrow r > \frac{t_{n-2}}{\sqrt{n-2+t_{n-2}^2}} \qquad (1)$$

237   indicates when the correlation coefficient of the sample, r, is significant. n is the number of
238   points and t_{n-2} refers to the Student's t coefficient for $n-2$.
239   In our study, for the selected data, the correlation coefficient begins to be significant when it
240   is greater than 0.1453 (95% of confidence, from relation (1), with n>30), which occurs in all
241   the years studied, as shown by the time series in Figure 8.
242
243   There is an increase in correlation in the central part of the period studied, possibly due to
244   the harsh economic times and the subsequent effects on pollution following the 1970s energy
245   crisis. During this period of great visibility, natural sources such as humidity and wind were
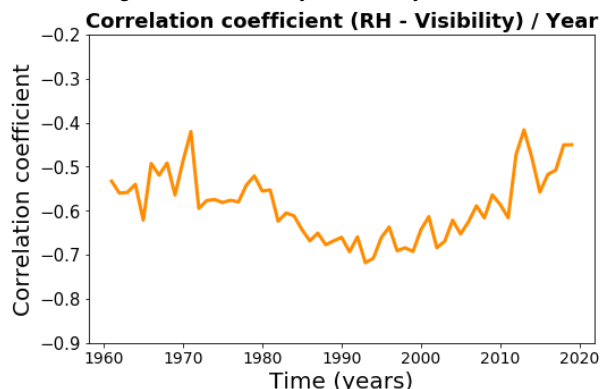246   more significant in accounting for the variability in visibility.

248   Figure 8: Correlation coefficient between annual relative humidity, RH, and visibility. The adjustment has been
249   made by taking the 3 daily visibility data and RH measurements.
250
251   As regards the contribution of the wind, the different correlations with visibility have been
252   calculated in the same way as for relative humidity. On this occasion, in addition, the long-
253   term trends (trending series) were removed from the visibility series because they were clearly
254   not related to the wind. In this way, it can be observed that the correlations for the entire period,
255   shown in Table 2, increased and stabilized, and were negative for wind from the ESE-SSW
256   sectors and positive from the NW directions, due to the different types of wind already
257   mentioned.
258
259   Table 2: Correlation coefficients between wind and visibility at 07:00 LT, 13:00 LT and 18:00 LT for the measurements taken
260   during the period 1961- 2019 in which the wind came from the NW or ESE-SSW directions, once long-term trends were removed.
261   Non-significant correlations are indicated by the sign "-".
262

January-March	April-June

	07 LT	13 LT	18 LT	07 LT	13 LT	18 LT
N-W	0.5	0.3	0.17	0.64	0.29	0.53
ESE-SSW	-	- 0.24	-	- 0.18	- 0.23	-
	July-September			October-December		
	07 LT	13 LT	18 LT	07 LT	13 LT	18 LT
N-W	0.72	0.43	0.55	0.60	0.36	0.44
ESE-SSW	- 0.24	- 0.20	-	- 0.30	- 0.24	-

263

5. Conclusions

265

266 Long-term variations in visibility over periods of years are the most important ones and may
267 be explained in terms of the concentration of aerosols, which saw a significant decrease in
268 Europe due to pollution mitigation measures at the end of the 20th century. In the last decade,
269 however, there has been a prevailing steep decline in visibility.

270

271 The study carried out by us using the local wind regime indicates a clear distinction between
272 the winds coming from the SSE-SSW sectors and those coming from the W-NW which, due
273 to the local orography, are the most predominant in the area. The SSE-SSW winds are less
274 intense yet more frequent in summer. They are associated with minimum visibility values, as
275 indicated by the negative correlation coefficient obtained when comparing the data of both
276 variables. However, the W-NW winds are the most intense ones recorded at the Observatory
277 site. They are more frequent in winter and are associated with maximum visibility.
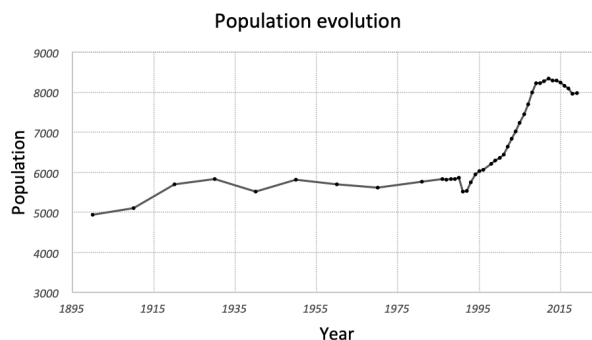

279 Figure 9: Variation of the population in the municipality of Roquetes, home to the Ebro Observatory, between
280 1900 and 2020.

281

282

283 Finally, and with the results obtained in the previous section, it can be concluded that, in the
284 short term, relative humidity and wind have a significant influence on visibility. However, in the
285 long term, other factors, which may include pollution, are more decisive. It is noteworthy that

286 from the year 2000 onward there has been a large increase in the population of the town of
287 Roquetes where the Ebro Observatory is located and where the measurements were taken
288 (Figure 9). Similar increases in population have been seen in neighbouring towns such as
289 Tortosa or Amposta, both within the scope of the visibility area we are studying. An increase
290 in industrial activity and/or the traffic this entails may be the reason that an increase in
291 pollutants was recorded and a corresponding reduction in visibility. As a conclusion, we can
292 affirm that the long-term variability of visibility at the Ebro Observatory as representative of the
293 Baix Ebre region cannot be explained by natural factors and, thus, other factors such as an
294 increase in man-made pollution should be taken into consideration.

6. Acknowledgments

295

296

7. References

303

304 Cardús, J.O. (1983). El Observatorio del Ebro, Memoria Num. 14, Sugrañes, Roquetes.

305

306 Cirera, R. (1906) «Noticia del Observatorio del Ebro y de algunas observaciones del eclipse
307 de 30 de Agosto de 1095», Memorias del Observatorio del Ebro nº 1, Barcelona, G. Gili Ed.

308

309 Cirera, R. (1910). Prólogo: El Observatorio del Ebro. Boletín mensual del Observatorio del
310 Ebro, vol. 1, p. 7-14.

311

312 Curto, J. J., Also, E., Pallé, E. and Solé, J. G. (2008). Sunshine and synoptic cloud
313 observations at Ebro Observatory, 1910-2006. Int. J. Climatol, vol. 28.

314

315 Deng, J., Du, K., Wang, K., Yuan, CS and Zhao J. (2012). Long-term atmospheric visibility
316 trend in Southeast China, 1973–2010, Atmospheric Environment, 59, 11-21,
317 10.1016/j.atmosenv.2012.05.023.

318

319 Doyle, M. and Dorling, S. (2002). Visibility trends in the UK 1950–1997, Atmospheric
320 Environment, 36(19), 3161-3172. https://doi.org/10.1016/S1352-2310(02)00248.

321

322 Founda, D., Kazadzis, S., Mihalopoulos, N., Gerasopoulos, E., Lianou, M., and Raptis, P. I.
323 (2016). Long-term visibility variation in Athens (1931–2013): a proxy for local and regional
324 atmospheric aerosol loads. *Atmospheric Chemistry and Physics*, *16*(17), 11219-11236.

325

326 García de Pedraza, L. and García Vega, J. (2013). Notas climáticas para un estudio
327 comparativo entre las cuencas de los ríos Po y Ebro. Agencia Estatal de Meteorología. p. 252-
328 255.

329

330 Hu, Y., Yao, L., Cheng, Z. and Wang Y. (2017), Long-term atmospheric visibility trends in
331 megacities of China, India and the United States, Environmental Res., 159:466-473. doi:
332 10.1016/j.envres.2017.08.018.

333

334 Lawal, B. (2014). Applied Statistical Methods in Agriculture, Health and Life Sciences, 115-
335 168, Springer. https://doi.org/10.1007/978-3-319-05555-8

336

337 López-Moreno, J. I., Vicente-Serrano, S. M., Moran-Tejeda, E., Zabalza, J., Lorenzo-Lacruz,
338 J., and García-Ruiz, J. M. (2011). Impact of climate evolution and land use changes on water
339 yield in the Ebro basin, Hydrol. Earth Syst. Sci.,15, 311–322, https://doi.org/10.5194/hess-15-
340 311-2011.

341

342 López-Moreno, J.I., Vicente-Serrano, S.M., Zabalza, J., Beguería, S., Lorenzo-Lacruz, J.,
343 Azorín-Molina, C. and Morán-Tejeda, E. (2013). Hydrological response to climate variability at
344 different time scales: A study in the Ebro basin, Journal of Hydrology, Volume 477, 175-188,
345 https://doi.org/10.1016/j.jhydrol.2012.11.028.

346

347 Molnár, A., Mészáros, E., Imre, K. and Rüll, A. (2002). Trends in visibility over Hungary
348 between 1996 and 2002, Atmospheric environment, 42(11):2621-2629, doi:
349 10.1016/j.atmosenv.2007.05.012.

350

351 Puig, I. (1927). El Observatorio del Ebro: Idea General Sobre el Mismo, Algueró y Baiges,
352 Tortosa,

353

354 Raso, J. M. (1987). Variaciones recientes de la temperatura media en el observatorio del Ebro.
355 Madrid, Anales Universidad Complutense, Volume 7,155-165.

356

357 Sabetghadam, S., Ahmadi-Givi, F. and Golestani Y. (2012). Visibility trends in Tehran during
358 1958–2008, Atmospheric Environment, 62:512–520, doi: 10.1016/j.atmosenv.2012.09.008.

359

360 Sloane, C.S., (1982). Visibility trends—II. Mideastern United States 1948—1978, Atmospheric
361 Environment, 1967 Vol. 16; Iss. 10, doi:10.1016/0004-6981(82)90117-2

362

363 Tsai, Y. (2005). Atmospheric visibility trends in an urban area in Taiwan 1961–2003,
364 Atmospheric environment, 39(30):5555-5567, doi: 10.1016/j.atmosenv.2005.06.012.

365

366 Vautard, R., Yiou, P., and Oldenborgh, G. (2009) Decline of fog, mist and haze in Europe over
367 the past 30 years, Nat. Geosci., 2, 115–119, doi:10.1038/ngeo414.

368

369 Vicente-Serrano, S. M. and Lopez-Moreno, J. I. (2006). Influence of atmospheric circulation
370 at different spatial scales on winter drought variability through a semi-arid climatic gradient in
371 Nort-east Spain, Int J. Climatol., 26(11), 1427–145

372

373 Vicente-Serrano, S. M., Beguería, S. and Lopez-Moreno, J. I., El Kenawy, A. M., and Angulo
374 M. (2009). Daily atmospheric circulation events and extreme precipitation risk in Northeast
375 Spain: the role of the North Atlantic Oscillation, Western Mediterranean Oscillation and
376 Mediterranean Oscillation, J. Geophys. Res., 114, D08106, doi:10.1029/2008JD011492.

Atmospheric
Chemistry
and Physics
Discussions

377

378   Vicente-Serrano, S. M., Camino, E. R., Castro, F. D. and Molina, C. A. (2017). An updated
379   review on recent trends in observational surface atmospheric variables and their extremes
380   over Spain. Cuadernos de Investigación Geográfica/Geographical Research Letters, 43, p.
381   209-232,

382

383   Wang, K., Dickinson, R. E. and Liang, S. (2009). Clear sky visibility has decreased overland
384   globally from 1973 to 2007, Science, 323(5920):1468–1470.

385

386   Wang, Y., Schmid. F. and Harou, A. (2010). Guide to the Global Observing System. Published
387   by: WMO.

388

389   World Meteorological Organization (1992). "Instrument and observing methods report".
390   Volume 46, 474, Geneva.